Supporting Information

Park et al. 10.1073/pnas.1214400109

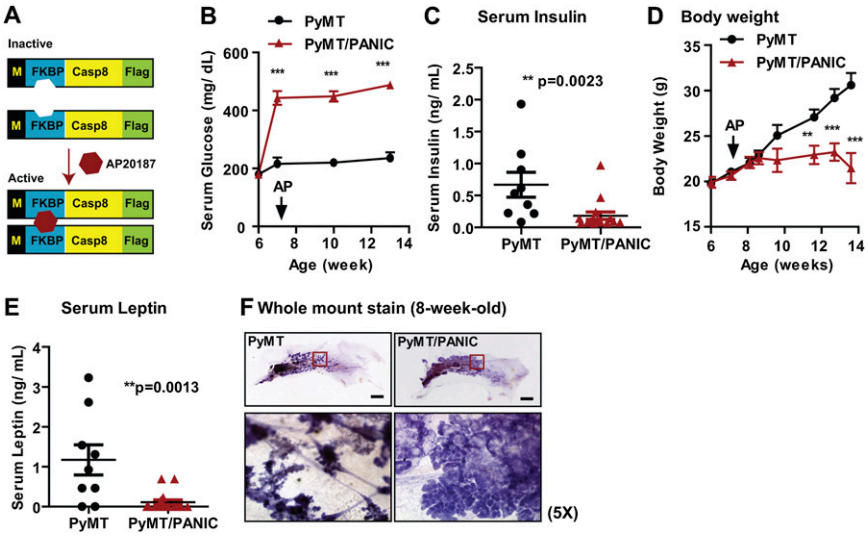

Fig. S1. Metabolic profiles of PyMT/PANIC mice compared with PyMT mice. (*A*) Schematic for the hyperglycemia induction in PANIC-ATTAC mice. Caspase8 cassettes are activated upon dimerize treatment (AP20187; Clontech). (*B*) Serum glucose levels (feeding condition) were determined for PyMT/PANIC compared with PyMT. Hyperglycemia in PyMT/PANIC was induced by AP20187 injection (0.5 μg/g, i.p., 5 d) and maintained over the tumor progression (n = 9–16 per group). ***$P < 0.001$ vs. PyMT by two-way ANOVA. (*C*) Serum insulin levels were significantly decreased in PyMT/PANIC compared with PyMT because of concomitant increase of serum glucose levels (n = 9–16 per group). **$P = 0.0023$ vs. PyMT by unpaired Student's t test. (*D*) Body weight was determined over the tumor progression (n = 9–16 per group). **$P < 0.01$ and ***$P < 0.001$ vs. PyMT by two-way ANOVA. (*E*) Serum leptin reflecting body fat mass was determined (n = 9–16 per group). **$P = 0.0013$ vs. PyMT by unpaired Student's t test. (*F*) Early-stage of tumor progression was determined by whole mount staining of mammary gland tissues at 8-wk-old PyMT/PANIC compared with PyMT. (Scale bars: 50 mm.) Higher magnification for squared boxes is presented in *Lower*.

A Cancer-related signaling pathways (PyMT/PANIC vs. PyMT)

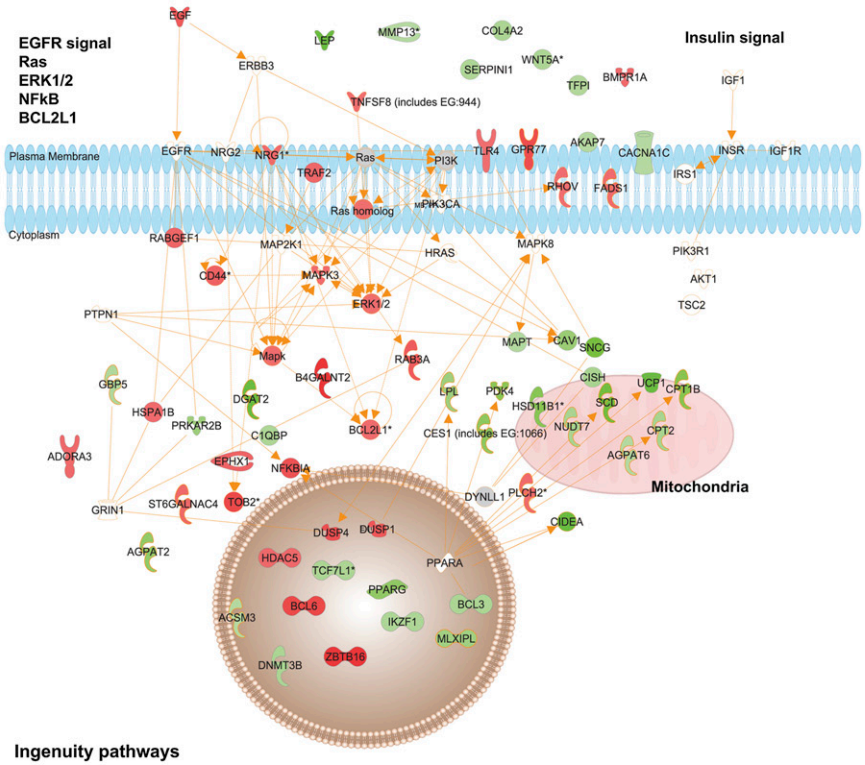

B

Pathway analysis	Gene (symbol)	Folds	p-value	Illumina ID
Increased	ATP2A3	1.770	1.87E-03	ILMN_2900462
EGF/ Ras pathway	BCL6	1.566	2.19E-03	ILMN_1230353
NF-kB pathway	GPR77	1.515	8.08E-04	ILMN_2671707
Bcl2L1 mediated-	NFκB1A	1.469	4.54E-04	ILMN_3001914
anti-apoptosis	GADD45G	1.424	3.82E-02	ILMN_2903945
Protein modification	DUSP1	1.421	7.21E-03	ILMN_2622983
- glycosylation	EGF	1.407	2.70E-02	ILMN_2684104
- disulfide	RAB26	1.355	3.70E-02	ILMN_2722058
- Ubl conjugation	RABGEF1	1.292	9.16E-03	ILMN_1226143
	CCRL2	1.250	2.45E-02	ILMN_2752624
	BCL2L1	1.224	2.24E-02	ILMN_2647885
Decreased	DGAT2	-5.246	2.72E-03	ILMN_1219915
lipid metabolism	LEP	-5.149	5.08E-03	ILMN_2695964
glucose metabolism	SCD	-2.968	1.29E-02	ILMN_1237375
ER function	COX8B	-2.942	1.43E-02	ILMN_2727520
Mitochondria function	CPT1B	-2.265	4.47E-02	ILMN_1227666
	HSD11B1	-2.211	2.54E-02	ILMN_2774160
	PFK4	-2.177	3.89E-02	ILMN_1259322
	PPARγ	-2.002	1.19E-02	ILMN_1221060
	AGPAT2	-1.965	4.95E-02	ILMN_1217252
	CAV1	-1.798	3.51E-02	ILMN_2632665
	LPL	-1.672	4.27E-02	ILMN_2692723
	HK2	-1.625	3.10E-03	ILMN_1239397
	CPT2	-1.429	1.48E-02	ILMN_2885532
	DNMT3B	-1.389	4.36E-02	ILMN_1252310
	BCL3	-1.374	9.47E-03	ILMN_2749717

Fig. S2. cDNA microarray for tumor tissues of PyMT/PANIC mice compared with PyMT. (*A*) Cancer-related pathway analysis (Ingenuity), revealing that EGFR, Ras, ERK1/2, NF-κB, and BCL2-L1 pathways are up-regulated in tumor tissues of PyMT mice upon hyperglycemia challenge. (*B*) Molecules in pathway analysis. Highly up- or down-regulated genes by hyperglycemia are listed in the table.

A

	ID	Symbol	Entrez Gene Name
1	ILMN_3162594	ARHGAP15	Rho GTPase activating protein 15
2	ILMN_2814927	CHGA	chromogranin A (parathyroid secretory protein 1)
3	ILMN_2503552	CSMD1	CUB and Sushi multiple domains 1
4	ILMN_1251139	DENND4C	DENN/MADD domain containing 4C
5	ILMN_2653462	EFEMP1	EGF-containing fibulin-like extracellular matrix protein 1
6	ILMN_2716212	EFNB2	ephrin-B2
7	ILMN_2669766	EID1	EP300 interacting inhibitor of differentiation 1
8	ILMN_3131522	FBXO3	F-box protein 3
9	ILMN_1239397	HK2	hexokinase 2
10	ILMN_2572649	KDR	kinase insert domain receptor (a type III receptor tyrosine kinase)
11	ILMN_1243671	MAST4	microtubule associated serine/threonine kinase family member 4
12	ILMN_3162138	MIIP	migration and invasion inhibitory protein
13	ILMN_2605307	MTMR10	myotubularin related protein 10
14	ILMN_1227012	NDUFB4	NADH dehydrogenase (ubiquinone) 1 beta subcomplex, 4, 15kDa
15	ILMN_2971688	NRG1	neuregulin 1
16	ILMN_2860174	PFKFB3	6-phosphofructo-2-kinase/fructose-2,6-biphosphatase 3
17	ILMN_2626470	PLB1	phospholipase B1
18	ILMN_1243525	PLDN	pallidin homolog (mouse)
19	ILMN_1221060	PPARG	peroxisome proliferator-activated receptor gamma
20	ILMN_1253819	PRKAR2B	protein kinase, cAMP-dependent, regulatory, type II, beta
21	ILMN_2636859	RBBP8	retinoblastoma binding protein 8
22	ILMN_2838501	SLC24A3	solute carrier family 24 (sodium/potassium/calcium exchanger), member 3
23	ILMN_1222499	SLC33A1	solute carrier family 33 (acetyl-CoA transporter), member 1
24	ILMN_1216265	TSHZ1	teashirt zinc finger homeobox 1
25	ILMN_2497067	ZMYND11	zinc finger, MYND domain containing 11

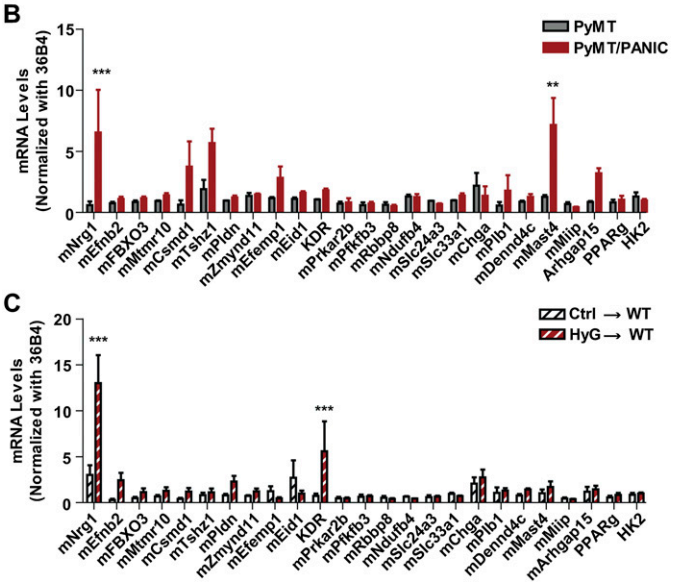

Fig. S3. Comparison microarray data with FAIRE-seq data. (*A*) List of candidate molecules. (*B*) Quantitative (qRT-PCR), revealing increased Nrg1 mRNA levels in tumor tissues of PyMT mice upon hyperglycemia challenge ($n = 8$ per group). ***$P < 0.001$, **$P < 0.01$ vs. PyMT by two-way ANOVA. (*C*) qRT-PCR, showing that consistent increase of Nrg1 mRNA levels in HyG tumors than Ctrl tumors ($n = 6$ per group). Results were normalized to 36B4 and represented as mean ± SEM ***$P < 0.001$ vs. Ctrl→ WT by two-way ANOVA.

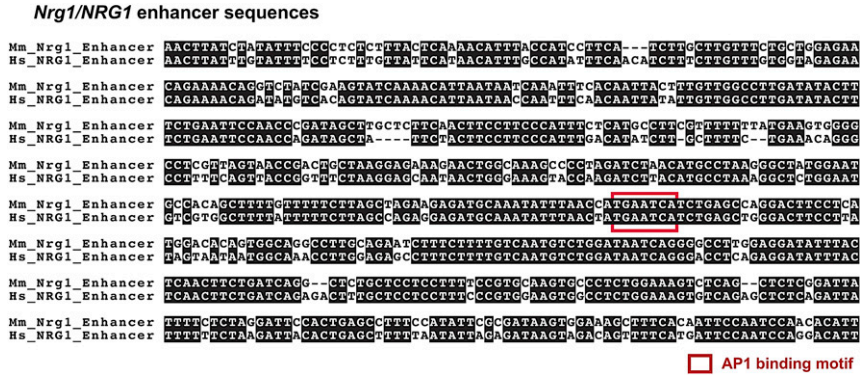

Fig. S4. Homology between mouse and human NRG1 enhancer sequences. Square indicates conserved AP-1 binding motif.

A Mouse Nrg1 mRNA sequences amplified in HyG-tumors compared to Ctrl-tumors

>uc009ljn.1_mm9_1_1 240 0 0 chr8:32928500 -32928739 -

ATGGACAGCAACCCAAGTTCTGTGAGCAGTAACTCAGAAAGTGAGACAGAAGATGAAAGAGTAGGTGAA
GATACACCATTCCTGGGCATACAGAACCCCCTGGCAGCCAGCCTTGAGGTGGCCCCTGCCTTCCGTCTGGCT
GAGAGCAGGACTAACCCAGCAGGCCGCTTCTCCACACAGGAAGAATTACAGGCCAGGCTGTCTAGTGTAAT
CGCTAACCAAGACCCTATTGCTGTATAA

B Homologous sequences in human NRG1 mRNA

>uc009ljn.1_hg18_1_1 240 0 0 chr8:32741223 -32741462 +

GTGGACAGCAACACAAGCTCCCAGAGCAGTAACTCAGAGAGTGAAACAGAAGATGAAAGA
GTAGGTGAAGATACGCCTTTCCTGGGCATACAGAACCCCCTGGCAGCCAGTCTTGAGGCAAC
ACCTGCCTTCCGCCTGGCTGACAGCAGGACTAACCCAGCAGGCCGCTTCTCGACACAGGAAG
AAATCCAGGCCAGGCTGTCTAGTGTAATTGCTAACCAAGACCCTATTGCTGTATAA

C Human NRG1 isoforms

Accession	Description	E-value	Max identity
NP_001153473.1	pro-neuregulin-1, isoform HRG-beta1d	1e-30	100%
NP_001153476.1	pro-neuregulin-1, isoform HRG-beta1c	2e-30	100%
NP_001153471.1	pro-neuregulin-1, isoform HRG-beta1b	3e-30	100%
NP_039250.2	pro-neuregulin-1, isoform HRG-beta1	4e-30	100%
NP_039251.2	pro-neuregulin-1, isoform HRG-beta2	5e-30	100%
NP_039258.1	pro-neuregulin-1, isoform HRG-alpha	9e-30	100%

Fig. S5. Mouse Nrg1 mRNA sequences amplified under hyperglycemic conditions and analogous human isoforms. RNA-seq analysis was performed with RNA samples subjected from the mouse HyG versus Ctrl tumors by the sequencing facility in the McDermott Center for Human Growth and Development, University of Texas Southwestern Medical Center. (Illumina Hi-Seq2000, SOLiD 5000xl). The murine Nrg1 isoforms have not yet been well defined, so a series of comparative alignments with human homologous are shown. (*A*) Mouse mRNA sequence up-regulated in HyG-tumors compared with Ctrl-tumors. (*B*) Human homologous sequences corresponding to mouse Nrg1 mRNA. (*C*) Blastx analysis (http://blast.ncbi.nlm.nih.gov) with human NRG1 homologous sequences indicates that several isoforms of heregulin are up-regulated in response to hyperglycemia.

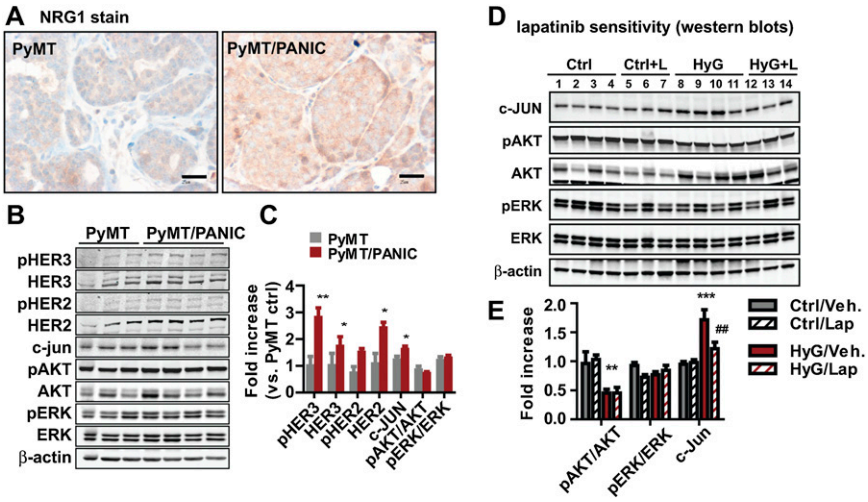

Fig. S6. Nrg1 acquisition in tumor tissues of PyMT/PANIC compared with PyMT. (*A*) Nrg1 immunostaining, showing higher Nrg1 signal in tumor tissues from PyMT/PANIC compared with those from PyMT mice. (Scale bars: 25 μm.) (*B*) Activation of HER receptors in tumors from PyMT/PANIC in comparison with those in PyMT. c-Jun levels were increased in PyMT/PANIC, whereas the effects on AKT and ERK activation was limited. β-actin was used as a loading control. (*C*) Quantified results for Western blots were normalized to β-actin and represented as mean ± SEM. Two independent cohort experiments were performed. $^{*}P < 0.05$, $^{**}P < 0.01$ vs. PyMT by two-way ANOVA. (*D*) Western blotting, showing an inefficient inhibition of AKT and ERK activation by a RTK inhibitor, lapatinib treatment (100 mg/kg per day by oral gavage) for both Ctrl and HyG tumor-bearing mice. c-Jun is consistently increased in HyG tumors compared with Ctrl tumors. β-actin was used as a loading control. (*E*) Quantified results represent as mean ± SEM, $n = 5$–6 per group. $^{**}P < 0.01$, $^{***}P < 0.001$ Ctrl-veh vs. HyG-veh; $^{\#}P < 0.05$, HyG-veh vs. HyG-lap by unpaired Student's *t* test.

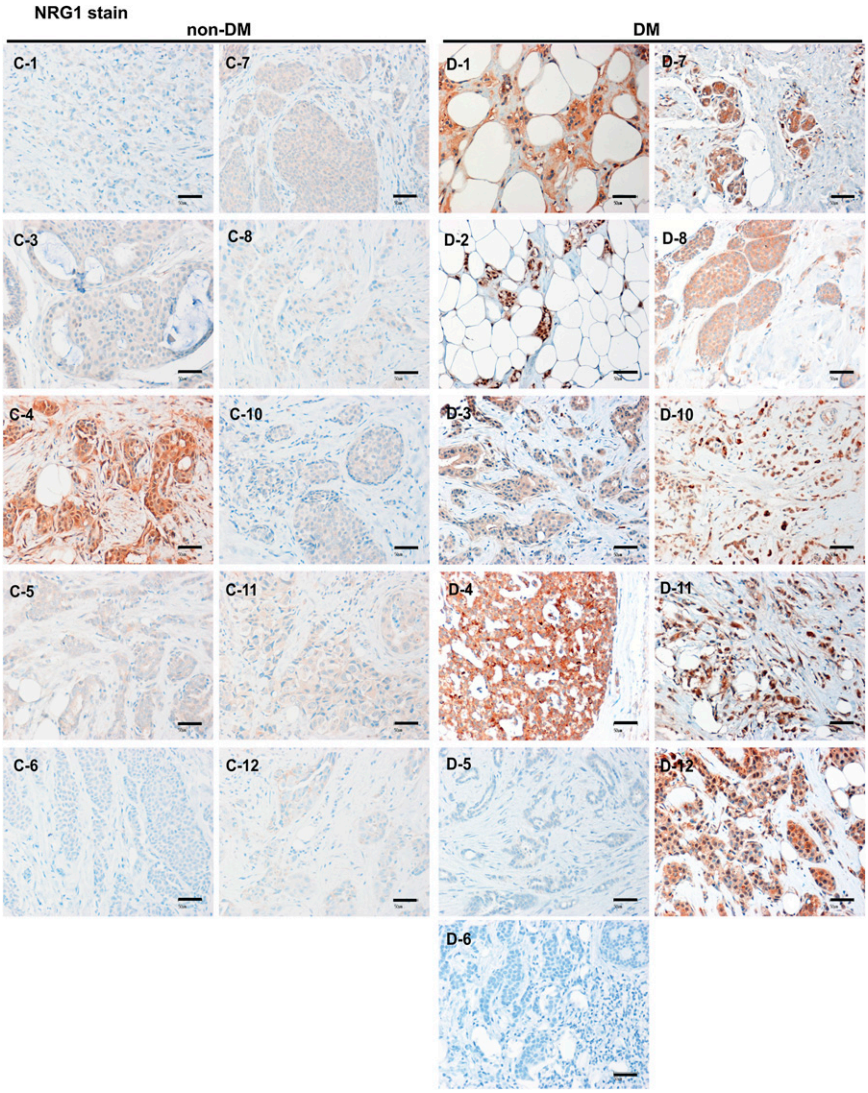

Fig. S7. NRG1 immunostaining for DM-diagnosed breast cancer patients compared with control patients. Paraffin-embedded tumor samples were immunostained with anti-NRG1 (H210; Santa Cruz Biotechnology). Hematoxylin was used for costaining. (Scale bars: 50 μm.)

Table S1. Fasting glucose levels and cancer marker status for human patients

Group	ID	Tumor grade	Glucose, mg/dL	NRG1	HER3	ER	PR	HER2	P53	Ki-67, %
Non-DM (n = 12)	C-1	1	87	0	0	+	—	—	—	12
	C-2	1	88	0	0	+	+	—	—	5
	C-3	1	89	0	0	+	+	—	—	7
	C-4	1	90	3+	0	+	+	—	—	9
	C-5	1	85	0	0	+	+	—	—	2
	C-6	1	88	0	2+	+	+	—	+	16
	C-7	1	84	0	0	+	+	—	—	47
	C-8	2	84	0	0	—	—	—	+	16
	C-9	2	84	0	0	+	+	—	—	18
	C-10	2	88	0	0	+	+	—	—	30
	C-11	3	85	0	0	—	—	—	+	54
	C-12	3	89	0	0	—	—	—	+	38
DM(n = 13)	D-1	1	145	2+	2+	+	—	—	—	10
	D-2	1	130	3+	0	+	+	—	+	9
	D-3	1	136	1+	0	+	—	—	—	14
	D-4	1	449	3+	1+	+	+	—	—	6
	D-5	1	163	0	0	+	+	—	—	20
	D-6	2	130	0	0	+	+	—	—	11
	D-7	2	201	1+	1+	+	+	—	—	5
	D-8	2	349	1+	0	+	+	—	—	14
	D-9	2	154	3+	2+	+	+	—	—	16
	D-10	2	184	3+	0	+	+	—	+	31
	D-11	2	194	2+	0	+	+	—	—	15
	D-12	2	370	2+	0	+	+	—	+	19
	D-13	2	135	3+	2+	+	+	—	—	28

HER2 negative, control (n = 12), and DM-diagnosed (n = 13) human breast cancer patient samples were included in this analysis. NRG1 and HER3 status were determined by immunohistochemistry. Scoring for NRG1 and HER3 staining intensity represents as 0 (negative) to 3 (strong). Other marker proteins such as ER (estrogen receptor), PR (progesterone receptor), HER2, p53, and Ki-67 were also assessed by immunohistochemistry. Specimens highlighted in red are represented in Fig. 5*A*.

Table S2. Primer sequences used in this study

Gene ID	Sense (5′ to 3′)	Antisense (5′ to 3′)
Arhgap15	AATCCAAGTTGTGGGTCCCTGGAG	TCAGTGCTCCGGTGACGACGT
Chga	CCGCCACCATCACCGCTGTT	GGGCAAAAACTTGCCCGGCG
Csmd1	CCCACTCGCTGGCTCTCTCTCCAG	GGATGGCTCCTCTCGGATGCG
Dennd4c	TGGGGAGCACACAGTCTTCGTCAG	TGCTCTTCAGGGGCGTGACCA
Efemp1	GGGGGCTTCCGCTGTTACCC	GGCAGCTCCCGGCACATAGTG
Efnb2	ACAGCGTCTTCTGCCCGCAC	CCTACCGTGTCCTCCCCGGG
Eid1	AGGTGTTCCTGCGAACCGCG	GGCTCTTCTCACACCGCGCC
FBXO3	TAGAGGCCGAGACGGGGCTG	TCCGAGGACACCTGGGCTCC
HK2	TGCCAAGCGTCTCCATAAGG	GGAGGAAGCGGACATCACAA
KDR	CAGACTGTGTCCCGCAGCCG	CACAGAGGCGGTATGCGCCC
Mast4	GGTTTAGCGGGAGAAGCCGCAG	TTGGACCACAGGAGCGCGTC
Miip	TTTCGGGCGGAGAGCGTTGG	CTAGCGGGACGAAGGCACGC
Mtmr10	CCGCCTCAGCACACCGACAG	TGCGGTGCTGCCTCAGCATC
Ndufb4	ACCAGAAGGGCGCAGGTCGA	CGACACGCGTTTGGGGTCGT
NRG1	TCCGGCAGAGCCTTCGGTCA	TCTCCCGTAGCCTCGGTGGC
Nrg1 (Type1)	GGGAATGAGCTGAACCGTAG	ACAATGGTGATGTTGGCAGA
Nrg1 (Type3)	TGCATTGCTGGCCTAAAGTG	GTTCTTCCGGGTGGGTACTG
Pfkfb3	ACCATTCAGACCGCGGAGGC	TCCGGGAGCTCTTCATGTTCTCTGA
Plb1	ATGGCATGGTGGGAACAGAAGCCAC	ACCGGGGACACACCTGGGTAC
Pldn	GCGCCCAGTGCGGGGATATG	TGTCGCTTAAGCCCGGCGTG
PPARg	CACAATGCCATCAGGTTTGG	GCTGGTCGATATCACTGGAGATC
Prkar2b	GCTGTGCTCGCTCTGCTGCTG	GTGCCTCAGCACCTCCACCG
Rbbp8	ACGGCAGCCTTACAACGCGG	ACCACGAGGGCTCTTGTGCAG
Slc24a3	TCCACCGCAAAGCGTCCGTG	TGTCGTCCCTCCGGGTTCCG
Slc33a1	AGCGACCAGTCTCTCCGCGT	GGGCCTGAGGCTGGCGTTTT
Tshz1	TTGTCAGGGTGACGTTGGCGAGA	CGGACATTCACTGGGTGGGCG
Zmynd11	AGCAAAGTGCCGAGCGGGTC	TGGAGGCGAGCACCGAGACA
EGFR	TGCCACCTATGCCACGCCAAC	ATCCCAAGGGCCACCACCACT
HER2	GCAACTGTGGTGGGCGTCCT	CAGCTCCACTGGGCGTCAGC
HER3	CACGGGGGCGTCAAACGTCA	GAGAGCGGGGTGACGGGAGT
CyclinD1	AGCCTCCAGAGGGCTGTCGG	GGCTGTGGTCTCGGTTGGGC
36B4	GGCATGCGGCCCGTCTCTC	CTTCCCTGGGCATCACGGCG
β-actin	CCACACCCGCCACCAGTTCG	TACAGCCCGGGGAGCATCGT